# Stream restoration can reduce nitrate levels in agricultural landscapes

Xiangqian Zhou[a,*], Seifeddine Jomaa[a], Xiaoqiang Yang[a], Ralf Merz[b], Yanping Wang[c], Michael Rode[a,d]

[a]Department of Aquatic Ecosystem Analysis and Management, Helmholtz Centre for Environmental Research - UFZ, Magdeburg, Germany

[b]Department of Catchment Hydrology, Helmholtz Centre for Environmental Research - UFZ, Halle (Saale), Germany

[c]School of Geographical Science, Nantong University, Nantong, China

[d]Institute of Environmental Science and Geography, University of Potsdam, Potsdam-Golm, Germany

[*]Corresponding author: Xiangqian Zhou (xiangqian.zhou@ufz.de)

## Abstract

The EU Water Framework Directive (WFD) has emphasized that altered stream/river morphology and diffuse pollution are the two major pressures faced by European water bodies at catchment scales. Increasing efforts have been directed toward restoration to meet WFD standards for ecological health, but this work has achieved limited success. One challenge is that little is known about how morphological changes (i.e., re-meandering) may affect nitrate retention within whole stream networks. We investigated this issue in the well-monitored Bode catchment (3,200 $km^2$) in central Germany. First, we implemented a fully distributed process-based mHM-Nitrate model, exploring its performance over the period from 2015 to 2018. Second, we simulated the effects of restoring more natural stream morphology (i.e., increasing sinuosity) on nitrate retention. The mHM-Nitrate model performed well in replicating daily discharge and nitrate concentrations (median Kling-Gupta values of 0.78 and 0.74, respectively). Within the stream network, gross nitrate retention efficiency was 5.1% and 67.2% in the winter and summer, respectively; this measure took into account both denitrification and assimilatory uptake. In the summer, the denitrification rate was about two times higher in a lowland sub-catchment dominated by agricultural lands than in a mountainous sub-catchment dominated by forested areas (204.1 and 102.4 mg N $m^{-2}$ $d^{-1}$, respectively). Similarly, in the same season, the assimilatory uptake rate was approximately five times higher in streams surrounded by lowland agricultural areas than in streams in higher-elevation, forested areas (200.1 and 39.1 mg N $m^{-2}$ $d^{-1}$, respectively). In the late summer, denitrification always peaked after assimilatory uptake. In our simulation, restoring stream sinuosity was found to increase net nitrate retention efficiency by up to 25.4%; greater effects were seen in small streams. Taken together, our results indicate that restoration efforts should consider augmenting stream sinuosity to increase nitrate retention and decrease nitrate concentrations at the catchment scale.

## Keywords:

River restoration; sinuosity; mHM-Nitrate model; stream denitrification; assimilatory uptake

## Highlights:

1. The denitrification rate and assimilatory uptake rate are higher in agricultural-dominant areas than in forest areas.

2. Increasing stream sinuosity improves net nitrate retention efficiency more in small streams than in large streams.
3. Small streams in agricultural areas should be given priority in restoration efforts.

# 1. Introduction

Excess nitrogen in surface waters represents a major threat to aquatic ecosystems (Birgand et al., 2007). In streams, inorganic nitrogen largely occurs in the form of nitrate ($NO_3^-$), a highly water soluble ion that can easily enter streams and rivers from both diffuse and point sources. To reduce nitrate levels in Europe's streams and rivers, extensive management strategies have been deployed over the past three decades (European Commission, 1991a; b). Their success remains limited, as around 60% of Europe's surface water bodies still have not attained ecological health (European Environment Agency,2018). The EU Water Framework Directive (WFD) has emphasized that, in Europe, altered stream/river morphology and diffuse pollution are two key pressures acting on water bodies at the catchment scale (Carvalho et al., 2019). For example, more than 37% of Germany's rivers are classified as heavily modified, as a result of channelization or straightening (Pander et al., 2017). The loss of stream bottoms has shortened water residence times and limited hyporheic exchanges, resulting in lower levels of nutrient retention and greater rates of downstream transport (Baker et al., 2012; Doyle et al., 2003; Gucker and Boechat, 2004; Opdyke et al., 2006). Attention has turned to stream restoration as a management tool for increasing nitrate retention (Craig et al., 2008; Newcomer Johnson et al., 2016; Wohl et al., 2015). Multiple techniques have been tested out in headwater streams and large lowland rivers (Flávio et al., 2017), such as re-meandering (Lorenz et al., 2009; Pedersen et al., 2014) and reconnecting streams with floodplains (Roley et al., 2012) and ponds (Passy et al., 2012) in agricultural zones.

Within streams, nitrate retention is the result of temporary retention by plants (i.e., assimilatory uptake) and permanent removal by bacteria (i.e., denitrification) (Groffman et al., 2009; Ye et al., 2012). In general, stream restoration is thought to promote both processes (assimilatory uptake: Huang et al. 2022; denitrification: Craig et al., 2008). To date, research has largely focused on the effects of re-meandering at the reach scale and has found contrasting results (Bukaveckas, 2007; Craig et al., 2008; Kaushal et al., 2008; Klocker et al., 2009; Lin et al., 2021; Veraart et al., 2014; Wagenschein and Rode, 2008). For example, denitrification was seen to be higher in restored streams (i.e., after reconnection with floodplains) than in unrestored streams (Kaushal et al., 2008; Roley et al., 2012). Furthermore, restored reaches may display higher levels of gross primary productivity and ecosystem respiration (Kupilas et al., 2017). In contrast, Klocker et al. (2009) found no difference in denitrification rates between restored and unrestored streams, and Veraart et al. (2014) observed that denitrification rates were highly variable: for some streams, rates were significantly higher in unrestored versus restored sections, while, in other streams, rates did not vary among sections. The researchers attributed these results to differences in hydrological conditions and levels of sedimentary organic matter. Thus, we presently have a limited understanding of how restoration could affect nitrate retention at broader scales.

Within stream networks, nitrate retention is shaped by complex interactions between hydrological, geomorphological, and biogeochemical processes (Ensign and Doyle, 2006; Yang et al., 2019; Ye et al., 2012). While the effects of hydrological and biogeochemical processes have been explored to some degree (Alexander et al., 2009; Covino et al., 2010; Marcé et al., 2018), there has been no systemic research on networks with contrasting morphologies and, more notably, on the effects of restoration efforts (i.e., re-meandering). This gap in knowledge likely results from three key challenges. First, it is difficult to disentangle how nitrate retention is affected by geomorphology versus other factors (Lin et al., 2016). Second, we lack detailed historical information on stream morphology (i.e., natural conditions) within catchments (Guzelj et al., 2020). Third, uncertainty arises when attempts are made to parse out the influences of lateral terrestrial flows versus in-stream processes (Helton et al., 2018; Helton et al., 2011).

Scenario analysis holds promise for addressing these challenges because it can be implemented by combining fully distributed catchment modeling with detailed spatiotemporal data from monitoring programs. In particular, simulations can explore how re-meandering could affect nitrate retention at the network scale. Recently, Yang et al. (2018) developed a fully distributed grid-based hydrological nitrate model (mHM-Nitrate) that can provide detailed spatial information on terrestrial nitrate inputs within stream networks. This model has successfully described terrestrial and aquatic processes (i.e., assimilatory uptake) (Yang et al., 2019) across different catchments (Wu et al., 2022; Yang et al., 2018; Zhou et al., 2022). In addition, researchers have been extensively characterizing the denitrification rates associated with different land-use types (Böhlke et al., 2009; Mulholland et al., 2009). This has yielded abundant opportunities for evaluating how morphological changes in streams can spatially and temporally impact nitrate transport and retention.

Here, we looked at how stream morphology affects spatiotemporal nitrate retention dynamics within a stream network—the Bode catchment in central Germany. To this end, we used the mHM-nitrate model, which can handle large gradients in catchment characteristics. More specifically, we aimed to i) evaluate assimilatory uptake and denitrification within the entire catchment; ii) characterize spatiotemporal variability in retention dynamics and identify the key factors at play in two sub-catchments; and iii) simulate the effects of re-meandering on nitrate concentrations and retention efficiency for a stream network.

# 2. Study area and methods

## 2.1 Study area

Covering around 3,200 km² in central Germany, the Bode catchment is closely monitored and thus serves as a rich source of hydrological and hydrochemical data (Mueller et al., 2016; Wollschläger et al., 2016). The catchment extends from the Harz Mountains, a low, rocky mountain range, to the northeastern lowlands of central Germany. Annual precipitation follows an elevational gradient within the catchment, ranging from more than 1,500 mm in the upper Harz Mountains to less than 500 mm in the vast lowland plains (Figure 1a). Mean annual air temperature ranges from 5 °C at Brocken, the mountain's highest peak, to 9.5 °C in eastern Magdeburg Börde (Wollschläger et al., 2016). The Harz Mountains have steep slopes with shallow, less fertile soils that are predominantly covered by forests.

All agricultural activity is associated with the region’s plateaus and lower-elevation areas. Within the catchment, 66% of the land is arable; 26% is forested or composed of semi-natural habitat; 7% is urban or dedicated to open-cast mining; and 1% is covered by water bodies and wetlands (CORINE 2012 land cover map, https://gdz.bkg.bund.de/index.php/default/open-data.html, last accessed 1 June 2020; Figure 1b).

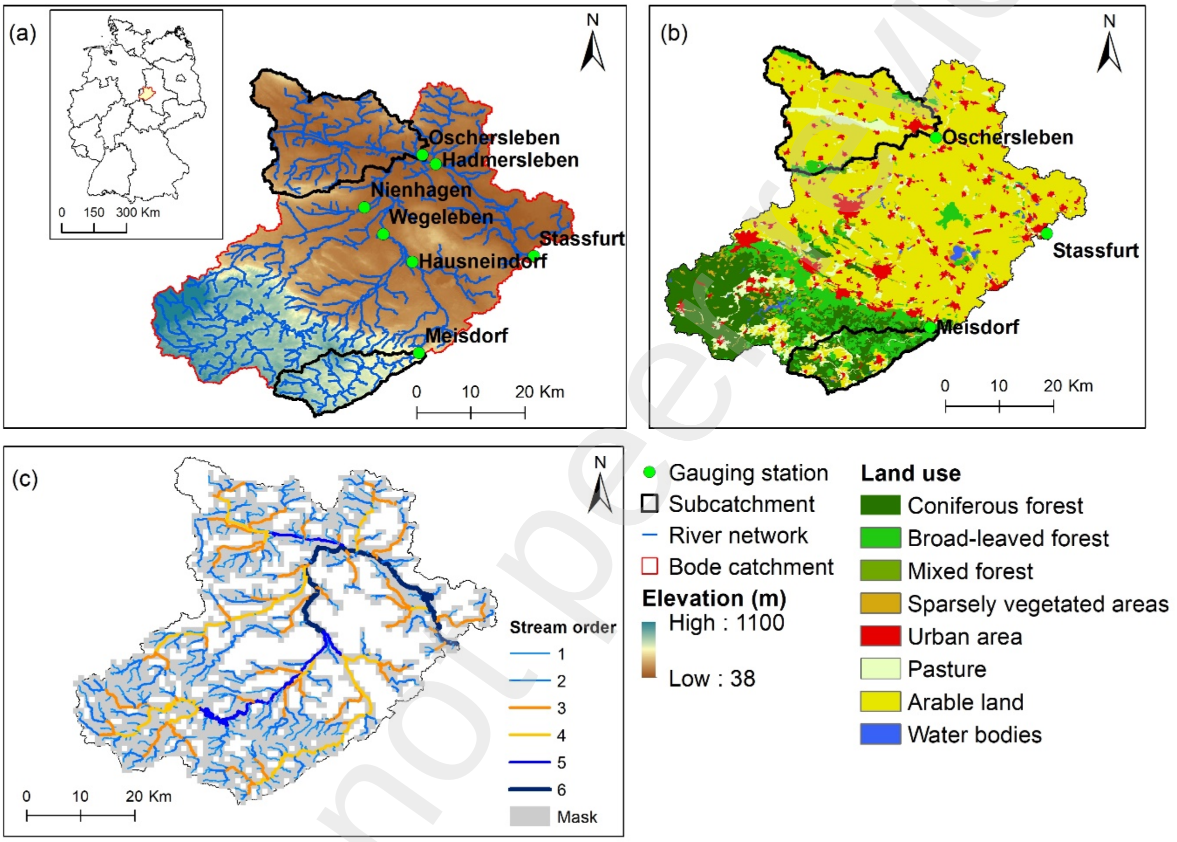


**Figure 1.** Bode catchment: (a) elevational map showing the gauging stations, (b) land use map, and (c) stream order obtained from the mHM-Nitrate model (1-km routing grid) with a stream mask derived from the observed network.

We chose two sub-catchments with different representative landscapes to investigate retention processes in greater detail. Upper Selke is a sub-catchment located in the Harz Mountains (Meisdorf outlet; Figure 1); it is dominated by forests (73% of 177.7 $km^2$) and contains natural streams. Großer Graben is a sub-catchment in the intensively farmed lowlands (Oschersleben outlet; Figure 1); it is dominated by arable land (87.4% of 435.4 $km^2$) and contains heavily modified streams (Figure 1b).

About 80% of the lowland stream network is heavily modified or completely changed (State Agency for Flood Protection and Water Management of Saxony-Anhalt, LHW; http://gldweb.dhi-wasy.com/gld-portal/, last accessed 10 April 2020; Figure S1). Stream order analysis showed that there were two times more streams in Großer Graben than in Upper Selke (Table S1), the result of artificial drainage in the former. Additionally, the total stream length in Großer Graben was twice that in Upper Selke, except in the case of 1st-order streams (Table S1). Small streams ($1^{st}$–$3^{rd}$ order) accounted for a high percentage of total stream length: 81% and 88% in Großer Graben and Upper Selke, respectively.

Mean daily nitrate concentrations (data collected at 15-min intervals) were available for the Meisdorf, Hausneindorf, Hadmersleben, and Stassfurt stations (Helmholtz Centre for Environmental Research – UFZ; Rode et al., 2016). Monthly and biweekly nitrate data (obtained via grab samples) were available for the Wegeleben, Nienhagen, and Oschersleben stations (LHW, http://gldweb.dhi-wasy.com/gld-portal/, last accessed 10 April 2020). Daily discharge data were available for all seven stations (LHW, http://gldweb.dhi-wasy.com/gld-portal/, last accessed 10 April 2020). Monthly nitrate concentrations were available for the Wegeleben and Nienhagen stations between 2007 and 2014. For the Wegeleben station, nitrate concentrations were unavailable in 2015 and between 2017 and 2018. However, they were available at two-month intervals at the Nienhagen station from 2015 to 2018 and at monthly intervals at the Oschersleben station from 2010 to 2018.

## 2.2 mHM-Nitrate model

The mHM-Nitrate model is a fully distributed process-based model of nitrate dynamics at the catchment scale (Yang et al., 2018). It was developed from the mesoscale Hydrological Model (Samaniego et al., 2010) and the Hydrological Predictions for the Environment model (Lindström et al., 2010). The mHM-Nitrate model simultaneously characterizes the hydrological and nitrate processes associated with terrestrial and stream environments for individual grid cells using a daily time step. For the terrestrial environment, the model considers the following key hydrological processes: interception, snow accumulation, snow melting, evapotranspiration, infiltration, groundwater recharge, and runoff generation. The nitrate processes considered are the sources of nitrate (i.e., wet atmospheric deposition, application of fertilizer and manure, and presence of plant/crop residues), transports (i.e., infiltration through multiple soil layers and percolation to the deep groundwater layer), sinks (i.e., denitrification and uptake by plants/crops), and transformation among the four nitrogen pools (i.e., dissolved inorganic nitrogen, dissolved organic nitrogen, active solid organic nitrogen, and inactive solid organic nitrogen) for each soil layer. For the stream environment, the model considered nitrate transformation (i.e., denitrification, assimilatory uptake, and remineralization) for each reach. More detailed descriptions of the mHM-Nitrate model can be found in Yang et al. (2018) and Yang et al. (2019); the source code can be found in Yang and Rode (2020).

Gross nitrate assimilatory uptake within streams ($F_{assim}$; kg N d$^{-1}$) was calculated using the new regionalization approach proposed by Yang et al. (2019):

$$F_{assim} = U_{assim} \times f_L \times W \times L \times H \times \Delta t \quad (1)$$

where $U_{assim}$ is the assimilatory uptake rate (mg N $m^{-3}$ $d^{-1}$); $f_L \in$ [0,1] is a light availability coefficient that reflects the combined impact of global radiation and riparian shading on assimilatory uptake; and $W$, $L$,$H$ are stream width (m), length (m), and depth (m), respectively.

Net assimilatory uptake within streams ($F_{net}$; kg N d$^{-1}$) was calculated by subtracting remineralization from gross assimilatory uptake (Yang et al., 2019), which was determined by multiplying gross assimilatory uptake and a temperature factor ($f_T$),

$$F_{net} = F_{assim} \times f_T \times f_{net} \quad (2)$$

$$f_T = \frac{T}{20} \times \frac{T_{10} - T_{20}}{5} \quad (3)$$

where $f_{net} \in$ [0,1] is a land-use coefficient that reflects the fraction of gross assimilatory uptake; $T$ is water temperature (°C); and $T_{10}$ and $T_{20}$ are mean water temperature at 10 and 20 days, respectively.

The amount of denitrification within streams ($F_{den}$; kg N d$^{-1}$) was calculated based on the relationship between the denitrification rate and nitrate concentrations:

$$F_{den} = U_{den} * W * L \tag{4}$$

$$U_{den} = U_{max} * \frac{C_{NO_3^-}}{C_{NO_3^-} + ks} * f_{temp} \tag{5}$$

$$f_{temp} = \begin{cases} 0 \quad , & T < 0 \\ \frac{T}{5} \times 2^{\frac{T-20}{10}}, & 0 < T < 5 \\ 2^{\frac{T-20}{10}} \; , & T > 5 \end{cases} \tag{6}$$

where $U_{max}$ is the maximum potential denitrification rate (mg N m$^{-2}$ d$^{-1}$) and $U_{den}$ is the denitrification rate (mg N m$^{-2}$ d$^{-1}$) adjusted for $C_{NO_3^-}$ (nitrate concentration; mg N L$^{-1}$) and $ks$ (nitrate concentration at half saturation; mg N L$^{-1}$). The latter has a default value of 1.5 mg N L$^{-1}$ in the mHM-Nitrate model (Yang et al., 2018).

The net nitrate retention efficiency ($Eff_{net}$) of a stream is the amount of nitrate retained by net assimilatory uptake and denitrification (sum of $F_{den}$ and $F_{net}$) divided by the total nitrate input load ($L_{input}$; the sum of lateral terrestrial imports and upstream loads). The gross nitrate retention efficiency ($Eff_{gross}$) for a stream is the amount of nitrate retained by gross assimilatory uptake and denitrification (sum of $F_{den}$ and $F_{assim}$) divided by the total nitrate input load ($L_{input}$) (Wollheim et al., 2008).

In previous studies using the mHM-Nitrate model, stream networks were generated using the digital elevation model (DEM), and nitrate retention processes within streams (both assimilatory uptake and denitrification) were considered for all reaches (i.e., grid cells). This approach may generate a high degree of uncertainty around retention levels because of the uncertainty around the quantity of benthic surface area within the stream network. Thus, we employed a high-resolution digital elevation model (DEM; 25 × 25 m) in combination with the observed stream network (LHW, http://gldweb.dhi-wasy.com/gld-portal/, last accessed 10 April 2020) (Figure 1c) to generate a more representative model stream network.

To this end, we first created a fishnet grid polygon with a routing resolution of 1 × 1 km using the Create Fishnet tool in the Data Management Toolbox in ArcMap 10.8. Second, the fishnet polygon was transposed onto the observed stream network (Figure 1c). If the real stream occurred within a grid cell of the fishnet polygon, the grid cell was assigned a value of 1; if not, the grid cell was assigned a value of 0. Third, the fishnet was converted to raster using the Polygon to Raster tool in the Conversion Toolbox and exported into an ASCII file using the Raster to ASCII tool, also in the Conversion Toolbox. Fourth, the ASCII file was imported into the mHM-Nitrate model, where the routing source code was modified to consider an additional routing mask—representing the observed stream network. Stream retention processes were only activated within the routing mask (Figure 1c).

## 2.3 Model setup

We only briefly summarize the setup of the mHM-Nitrate model for the Bode catchment because it is described in detail elsewhere (Zhou et al., 2022). The model was run using daily time steps over the period from 2006 to 2018. It was calibrated using data from 2010 to 2014. The results were validated using data from 2015 to 2018, namely discharge and nitrate concentrations at seven gauging stations that reflected key features of the Bode catchment (e.g., land use, stream order, and nitrate concentration). To model processes within terrestrial and stream environments, the grid resolution was set to 1 km. To calibrate the model, we used sensitivity analysis to identify the 15 most sensitive parameters—the top 10 hydrological parameters and the top 5 nitrate parameters. The latter were the stream denitrification rate, the soil denitrification rate in arable and non-arable areas, and the assimilatory uptake rate within streams in arable and non-arable areas. The range for the assimilatory uptake rate (100–500 mg N $m^{-2}$ $d^{-1}$) was defined using high-frequency sensor measurements from previous research (Rode et al., 2016; Yang et al., 2019). The range for the stream denitrification rate (10–700 mg N $m^{-2}$ $d^{-1}$) was defined using studies on lowland streams in central Germany (Huang et al., 2022; Kunz et al., 2017a; Kunz et al., 2017b; Zhang et al., 2023).

## 2.4 Simulating stream restoration

We designed a model scenario to explore the effects of stream sinuosity on nitrate retention. It simulated a situation in which the current stream network had been restored, such that its sinuosity was greater than that seen in networks of channelized streams. Stream sinuosity ($S_n$) in each grid cell was calculated by dividing stream length (determined from LHW data) by thalweg length (determined using the DEM). We estimated the sinuosity of natural streams using a series of equations. First, we calculated stream power ($SP$; kg m s$^{-3}$) in each grid cell as follows (Rhoads, 2010):

$$SP = \rho g Q S \quad (7)$$

where $\rho$ is water density (1,000 kg m$^{-3}$), $g$ is the gravitational acceleration (9.8 m s$^{-2}$), $Q$ is the discharge rate (m$^3$ s$^{-1}$), and $S$ is the channel slope.

Second, we calculated natural stream sinuosity for the grid cells in which stream power was greater than 10 kg m s$^{-3}$. We drew on the work of Harnischmacher (2007), which showed that the sinuosity of lowland streams was correlated with stream power when stream power was between 10 and 100 kg m s$^{-3}$ (correlation coefficient = 0.946, p=0.001). This analysis used data for 11 undisturbed stream sections that served as references; these streams displayed similar geological conditions to natural streams in the lower Bode catchment (Harnischmacher, 2007). Sinuosity ($S_n$) was calculated as follows:

$$S_n = 0.043 + \ log_{10}^{SP} \quad (8)$$

For grid cells in which stream power was less than 10 kg m s$^{-3}$, we calculated natural stream sinuosity by estimating mean potential sinuosity based on stream type (Briem et al., 2003; Ministerium für Umwelt und Naturschutz Landwirtschaft und Verbraucherschutz des Landes Nordrhein-Westfalen, 2010). The lowlands of the Bode catchment are largely characterized by small loess and loam-dominated rivers (Type 18) (Figure S2), and potential natural sinuosity within the entire stream network ranges from 1.01 to 2.0, depending on stream type (Table S2). To simplify our calculations, we used the mean potential natural sinuosity for each stream type. Finally, we only focused on simulating the restoration of streams in arable areas, since the streams in forested areas were less affected by human activity (Figure S1). The riparian zone was sufficiently large in the lowland arable areas to allow for increases in stream sinuosity.

In the baseline scenario (i.e., the actual state of the Bode stream network), stream sinuosity was low (mean = 1.04 for 1st–3rd order streams and mean = 1.07 for 4th–6th order streams; Table 1). However, there was a certain degree of variability (range: 1.00–2.73), with high levels of sinuosity seen exclusively in very short stream sections (Figure S3a). In the restoration scenario, mean sinuosity increased by 0.35 relative to the baseline, with the biggest augmentation seen in 6th-order streams (Table 1 and Figure S3b).

The effects of stream restoration were simulated over the validation period because the years between 2015 and 2022 were relatively dry and warm (Zhou et al., 2022), which likely represents future conditions under climate change (Huang et al., 2015).

**Table 1**. Stream sinuosity range (and mean) for each stream order in the baseline and restoration scenarios.

| Stream order | Sinuosity | |
|---|---|---|
| | Baseline | Restoration |
| 1st | 1.00–2.53 (1.03) | 1.00–2.53 (1.30) |
| 2nd | 1.00–2.60 (1.04) | 1.00–2.60 (1.34) |
| 3rd | 1.00–2.28 (1.04) | 1.00–2.53 (1.44) |
| 4th | 1.00–2.73 (1.06) | 1.00–3.11 (1.50) |
| 5th | 1.00–2.09 (1.08) | 1.00–2.54 (1.29) |
| 6th | 1.00–2.65 (1.07) | 1.00–3.62 (1.55) |

# 3. Results

## 3.1 Model performance

The mHM-Nitrate model generally performed well when simulating discharge, nitrate concentrations, and nitrate loads at the seven gauging stations (Figure 2 and S4-S5 and Table 2). Nash-Sutcliffe efficiency (NSE) exceeded 0.72 and 0.80 for the calibration and validation periods, respectively (Table

2). For the validation period, the ranges of Kling-Gupta efficiency (KGE) were 0.52–0.93, 0.22–0.80, and 0.60–0.91 for discharge, nitrate concentrations, and nitrate loads, respectively (Table 2). The model did overestimate nitrate concentrations at the Oschersleben station (Figure 2d) for the whole modeling period (2010–2018); percent bias (PBIAS) was 11.0% and 28.8% for the calibration and validation periods, respectively. In contrast, nitrate loads were accurately estimated at all seven stations during both the calibration and validation periods (PBIAS range = -18.7–23.2%).

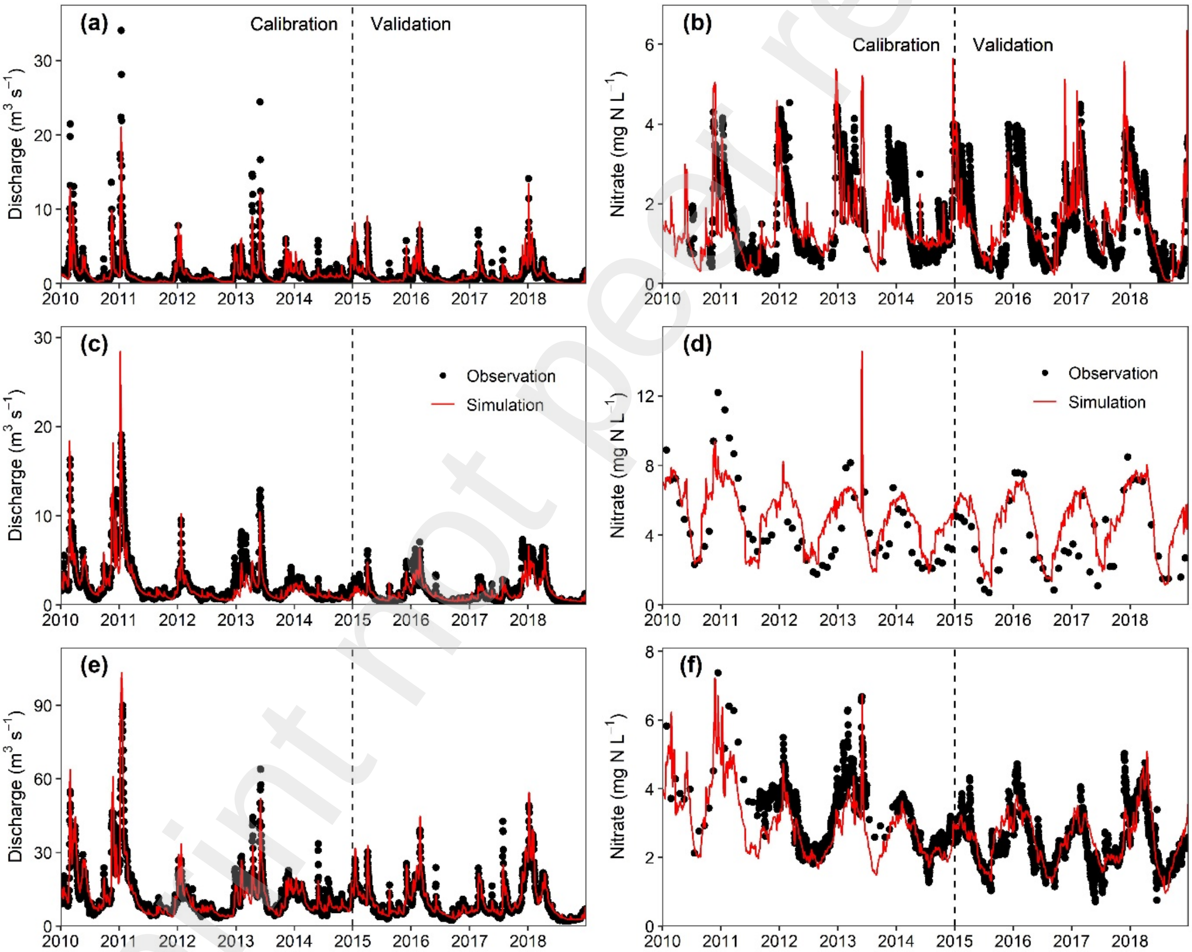


**Figure 2**. Performance of the mHM-Nitrate model: discharge and nitrate concentrations at (a-b) Meisdorf, (c-d) Oschersleben, and (e-f) Stassfurt during the calibration period (2010–2014) and validation period (2015–2018).

**Table 2**. Model evaluation metrics for daily discharge (Q; $m^3 s^{-1}$), nitrate concentrations (mg N $L^{-1}$), and nitrate loads (kg N $d^{-1}$) at the seven gauging stations during the calibration and validation periods. Metric abbreviations: NSE = Nash-Sutcliffe efficiency, KGE = Kling-Gupta efficiency, and PBIAS = percent bias.

| Station | Metric | Calibration (2010–2014) | | | Validation (2015–2018) | | |
|---|---|---|---|---|---|---|---|
| | | Q | $NO_3^-$ | Load | Q | $NO_3^-$ | Load |
| Meisdorf | NSE | 0.84 | 0.48 | 0.67 | 0.78 | 0.60 | 0.72 |
| | KGE | 0.77 | 0.70 | 0.74 | 0.71 | 0.76 | 0.82 |
| | PBIAS | 4.10 | -6.40 | -3.60 | 23.8 | 4.10 | 11.8 |
| Hausneindorf | NSE | 0.85 | -0.56 | 0.68 | 0.82 | 0.42 | 0.77 |
| | KGE | 0.87 | 0.44 | 0.75 | 0.78 | 0.72 | 0.83 |
| | PBIAS | 11.1 | -21.4 | 4.40 | 16.2 | 3.30 | 12.4 |
| Wegeleben | NSE | 0.93 | -0.36 | 0.79 | 0.93 | - | - |
| | KGE | 0.96 | 0.58 | 0.72 | 0.88 | - | - |
| | PBIAS | -0.50 | -17.0 | -16.2 | 3.30 | - | - |
| Nienhagen | NSE | 0.72 | -0.08 | 0.75 | 0.37 | -0.46 | 0.77 |
| | KGE | 0.80 | 0.50 | 0.78 | 0.52 | 0.22 | 0.70 |
| | PBIAS | 13.3 | -23.2 | -15.5 | 36.1 | -2.40 | 23.2 |
| Oschersleben | NSE | 0.75 | 0.54 | 0.65 | 0.80 | 0.41 | 0.78 |
| | KGE | 0.85 | 0.60 | 0.61 | 0.71 | 0.61 | 0.60 |
| | PBIAS | -8.70 | 11.0 | -13.3 | -8.30 | 28.8 | -10.7 |
| Hadmersleben | NSE | 0.87 | 0.52 | 0.85 | 0.93 | 0.61 | 0.93 |
| | KGE | 0.89 | 0.66 | 0.79 | 0.93 | 0.80 | 0.91 |
| | PBIAS | 0.80 | -8.30 | -8.50 | 4.80 | 6.30 | 5.80 |
| Stassfurt | NSE | 0.85 | 0.50 | 0.82 | 0.92 | 0.63 | 0.91 |
| | KGE | 0.87 | 0.71 | 0.72 | 0.91 | 0.80 | 0.91 |
| | PBIAS | 0.50 | -13.7 | -18.7 | 6.20 | 2.60 | 3.10 |

## 3.2 Spatiotemporal dynamics of nitrate retention

### 3.2.1 Annual and seasonal nitrate retention in the Bode catchment

The mHM-Nitrate model suggested that the Bode stream network experienced the highest total nitrate input loads ($L_{input}$) in the winter from 2015 to 2018 (annual mean = 3.68 kg N $ha^{-1}$ $y^{-1}$; Table 3). For this same period, annual net and gross nitrate retention efficiency ($Eff_{net}$ and $Eff_{gross}$) were 12.9% and 24.6%, respectively (Table 3). Both peaked in the summer (34.9% and 67.2%, respectively), which is when input loads were lowest and assimilatory uptake and denitrification were highest. In contrast, the two types of efficiency had lower values in the winter and spring (Table 3). Within the stream network, the assimilatory uptake rate ($U_{assim}$) reached its greatest value in the spring and summer (104.9 and 133.9 mg N m$^{-2}$ d$^{-1}$, respectively), while the denitrification rate ($U_{den}$) was highest in the summer and autumn (158.2 and 116.7 mg N m$^{-2}$ d$^{-1}$, respectively; Table 3).

**Table 3.** Variables describing mean annual and seasonal nitrate input loads and retention for the entire stream network from 2015–2018. Variable values were estimated using the mHM-Nitrate model; the only exception was $L_{obs}$, which was calculated from the observed data. Abbreviations: $L_{input}$ = total nitrate input load; $L_{obs}$ = observed exported nitrate load; $L_{out}$ = estimated exported nitrate load; $F_{assim}$ = amount of gross assimilatory uptake; $U_{assim}$ = assimilatory uptake rate; $F_{den}$ = amount of denitrification; $U_{den}$ = denitrification rate; $Eff_{net}$ = net nitrate retention efficiency; and $Eff_{gross}$ = gross nitrate retention efficiency.

| Variable | Winter | Spring | Summer | Autumn | Annual |
|---|---|---|---|---|---|
| $L_{input}$ (kg N ha$^{-1}$ season$^{-1}$/ kg N ha$^{-1}$ y$^{-1}$) | 1.49 | 1.06 | 0.52 | 0.56 | 3.68 |
| $L_{obs}$ (kg N ha$^{-1}$ y$^{-1}$) | 1.47 | 0.97 | 0.32 | 0.38 | 3.14 |
| $L_{out}$ (kg N ha$^{-1}$ y$^{-1}$) | 1.44 | 1.09 | 0.34 | 0.40 | 3.27 |
| $F_{assim}$ (kg N d$^{-1}$) | 58.1 | 565.7 | 512.7 | 165.5 | 321.0 |
| $U_{assim}$ (mg N m$^{-2}$ d$^{-1}$) | 12.7 | 104.9 | 133.9 | 45.9 | 74.7 |
| $F_{den}$ (kg N d$^{-1}$) | 169.7 | 320.9 | 536.7 | 362.1 | 348.4 |
| $U_{den}$ (mg N m$^{-2}$ d$^{-1}$) | 45.4 | 77.1 | 158.2 | 116.7 | 99.5 |
| $Eff_{net}$ (%) | 3.8 | 10.2 | 34.9 | 21.4 | 12.9 |
| $Eff_{gross}$ (%) | 5.1 | 27.7 | 67.2 | 31.2 | 24.6 |

### 3.2.2 Nitrate retention within two representative sub-catchments

For the period from 2015 to 2018, we investigated nitrate retention within two sub-catchments—Upper Selke and Großer Graben. They were chosen because they represented certain landscape profiles within the Bode catchment (Figure 1). To characterize daily rates of denitrification ($U_{den}$) and assimilatory uptake ($U_{assim}$), we determined the median values for all the streams in the network. Both rates were highly variable among seasons and years in the two sub-catchments (Figure 3).

At the annual scale, the denitrification rate ($U_{den}$) was nearly two times higher in Großer Graben than in Upper Selke (126.4 vs. 69.1 mg N $m^{-2}$ $d^{-1}$, respectively; Table 4). Seasonally, $U_{den}$ was high in the summer and autumn and low in the spring and winter in both sub-catchments (Figure 3 and Table 4). Furthermore, there was seemingly an influence of land-use type. In the summer, $U_{den}$ was two-fold greater in Großer Graben (median = 204.1 mg N $m^{-2}$ $d^{-1}$), which is dominated by arable land, than in Upper Selke, which is dominated by forests (median = 102.4 mg N $m^{-2}$ $d^{-1}$).

At the annual scale, the assimilatory uptake rate ($U_{assim}$) was more than three times higher in Großer Graben than in Upper Selke (102.0 vs. 27.6 mg N $m^{-2}$ $d^{-1}$, respectively; Table 4). This rate was also high in the spring and summer and low in the autumn and winter in both sub-catchments (Figure 3 and Table 4). In the summer, the $U_{assim}$ was five times greater in Großer Graben than in Upper Selke (median ± SD = 200.1 ± 27.1 vs. 39.1 ± 8.7 mg N $m^{-2}$ $d^{-1}$, respectively). In Upper Selke, it always peaked in April and then rapidly decreased (Figure 3a).

Compared to assimilatory uptake, denitrification accounted for a higher proportion of gross nitrate uptake in Upper Selke than in Großer Graben across all seasons, except for the spring (range in Upper Selke: 72–88% vs. Großer Graben: 51–87%; Table 4). A similar pattern was seen at the annual scale (Upper Selke: 71% vs. Großer Graben: 55%; Table 4).

Gross nitrate retention efficiency ($Eff_{gross}$) demonstrated clear annual and seasonal patterns in both sub-catchments (Figure 4); high values of $Eff_{gross}$ were seen during low-flow periods in the summer and autumn (Table 4). It decreased rapidly in July 2017 at Großer Graben and Upper Selke, the result of peak flow events causing high nitrate loads in streams (Figures 2a and 2c). At the annual scale, gross efficiency displayed a similar median value in both sub-catchments (Upper Selke: 26.0% and Großer Graben: 35.2%). In the summer, the median was higher for Großer Graben than for Upper Selke (82.2% vs. 58.8%, respectively). It is worth noting that the sub-catchments had similar median benthic surface areas in the summer (Großer Graben: 0.28 $km^2$ and Upper Selke: 0.24 $km^2$).

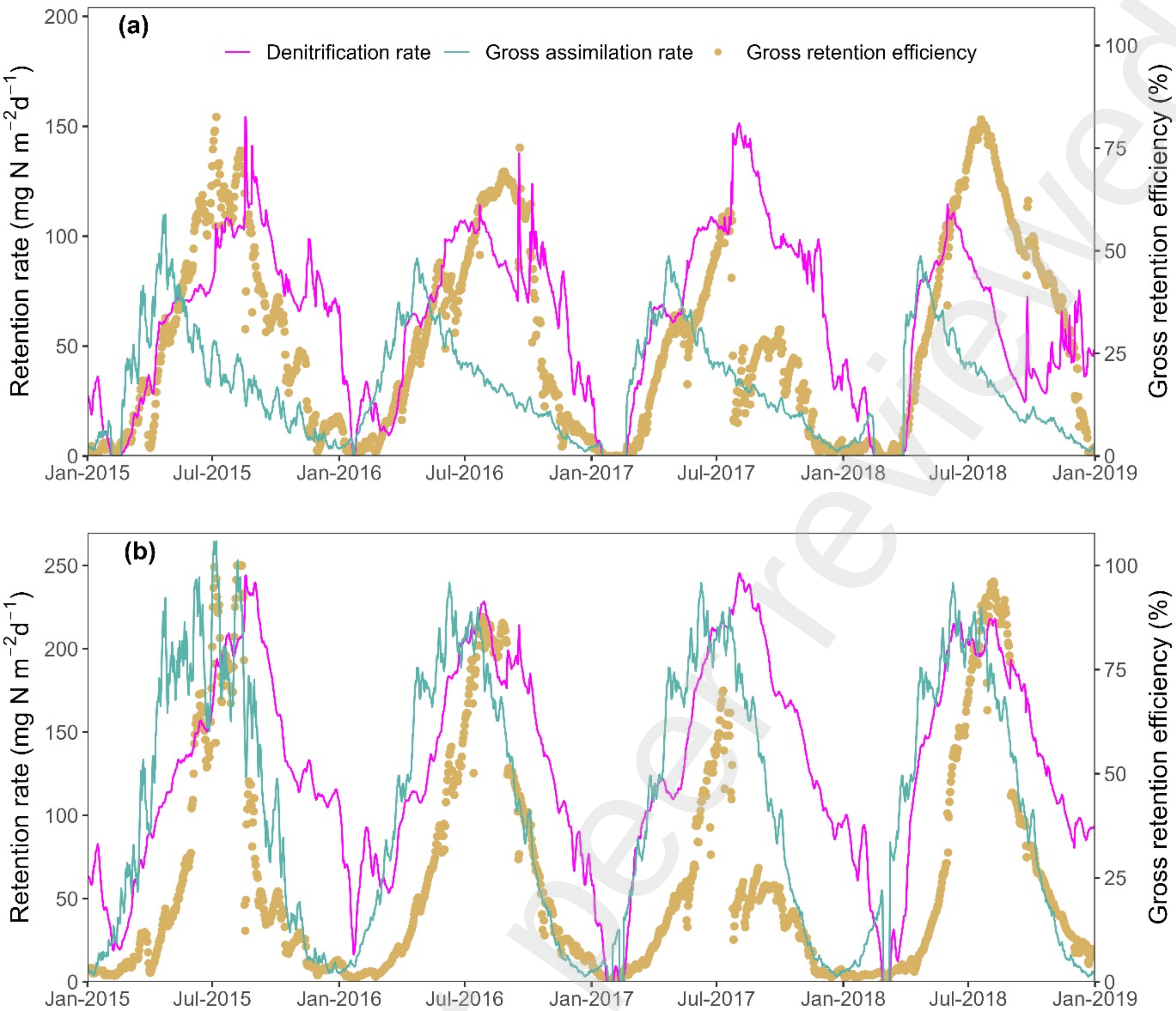


**Figure 3**. Daily denitrification rates, gross assimilation rates, and gross nitrate retention efficiencies in the sub-catchments of (a) Upper Selke and (b) Großer Graben from 2015 to 2018.

**Table 4**. Median ± SD daily denitrification rates, assimilatory uptake rates, and gross nitrate retention efficiency at seasonal and annual scales in the Upper Selke and Großer Graben sub-catchments from 2015 to 2018. Abbreviations: $U_{den}$ = denitrification rate; $U_{assim}$ = assimilatory uptake rate; and $Eff_{gross}$ = gross nitrate retention efficiency.

| Variable | Sub-catchment | Winter | Spring | Summer | Autumn | Annual |
|---|---|---|---|---|---|---|
| $U_{den}$ | Upper Selke | $25.9 \pm 22.8$ | $61.8 \pm 28.1$ | $102.4 \pm 22.1$ | $81.1 \pm 25.6$ | $69.1 \pm 36.5$ |
| (mg N m$^{-2}$ d$^{-1}$) | Großer Graben | $70.3 \pm 33.3$ | $111.1 \pm 41.3$ | $204.1 \pm 22.6$ | $148.9 \pm 34.8$ | $126.4 \pm 61.6$ |
| $U_{assim}$ | Upper Selke | $5.0 \pm 8.4$ | $63.9 \pm 22.7$ | $39.1 \pm 8.7$ | $18.3 \pm 6.1$ | $27.6 \pm 24.3$ |
| (mg N m$^{-2}$ d$^{-1}$) | Großer Graben | $9.9 \pm 14.7$ | $148.9 \pm 51.1$ | $200.1 \pm 27.1$ | $56.8 \pm 40.6$ | $102.0 \pm 77.5$ |
| $Eff_{gross}$ (%) | Upper Selke | $2.0 \pm 3.7$ | $22.7 \pm 14.0$ | $58.8 \pm 17.4$ | $29.3 \pm 17.2$ | $26.0 \pm 22.4$ |
| | Großer Graben | $5.4 \pm 7.0$ | $22.0 \pm 17.2$ | $82.2 \pm 23.3$ | $42.6 \pm 30.4$ | $35.2 \pm 31.7$ |

### 3.2.3 Spatiotemporal patterns in nitrate retention efficiency

We plotted accumulated net retention efficiency (ANRE) along an upstream to downstream gradient for the two main stems of the Upper Selke and Großer Graben sub-catchments (Figure 4: heatmap;

Figure S6: stream networks). ANRE is the ratio between total nitrate retention within streams and the total nitrate input load attributable to terrestrial sources. Spatiotemporal patterns in ANRE varied with catchment size, which increased from headwater to outlet. Dynamics were similar across seasons and years in both sub-catchments: ANRE was higher in the summer and autumn but lower in the winter and spring (Figure 4). ANRE remained high (>60%) between late June and late November of 2018 in Upper Selke and between late July and early December of 2018 in Großer Graben, periods of drought in the sub-catchments. Between 2015 and 2018, ANRE hit its minimum value in the summer of 2017, due to peak flows in July 2017 (Figure 4 and Figures 2a and 2c).

However, some differences were apparent between the two sub-catchments for the period between 2015 and 2018. In Upper Selke, which is dominated by forests, ANRE was lowest in headwater streams, as a result of their low assimilatory uptake rates ($U_{assim}$) and denitrification rates ($U_{den}$) (Figure 4a). In contrast, in streams near the outlet (<36 km away), ANRE reached high values (>60%) during the summer and autumn (Figure 4a). In Großer Graben, which is dominated by arable land, ANRE was highest in headwater streams, which experienced lower total nitrate input loads ($L_{input}$) than higher order streams (Figure 4b). In this sub-catchment, high ANRE values (>60%) only occurred in headwater streams that were about 40 km upstream from the outlet (Figure 4b).

In Upper Selke, there was a correlation between ANRE values in the summer and catchment size (Figure 4a). This pattern could have two explanations: 1) the relative surface area covered by forest increased from upstream to downstream and 2) there is a positive correlation between nitrate retention and benthic surface area. In the summer of 2018, ANRE was lower in the sub-catchment's middle region, namely in streams located 24.8 and 18.0 km from the outlet (Meisdorf station, Figure 4). Such was due to the large nitrate input loads ($L_{input}$) from nearby arable land (Figure S6a). Similarly, ANRE was dramatically lower in intermediate sections of Großer Graben (Figure 4b) because of the large nitrate input loads ($L_{input}$) from tributaries that joined the main network stem around 38.9 and 25.5 km from the outlet.

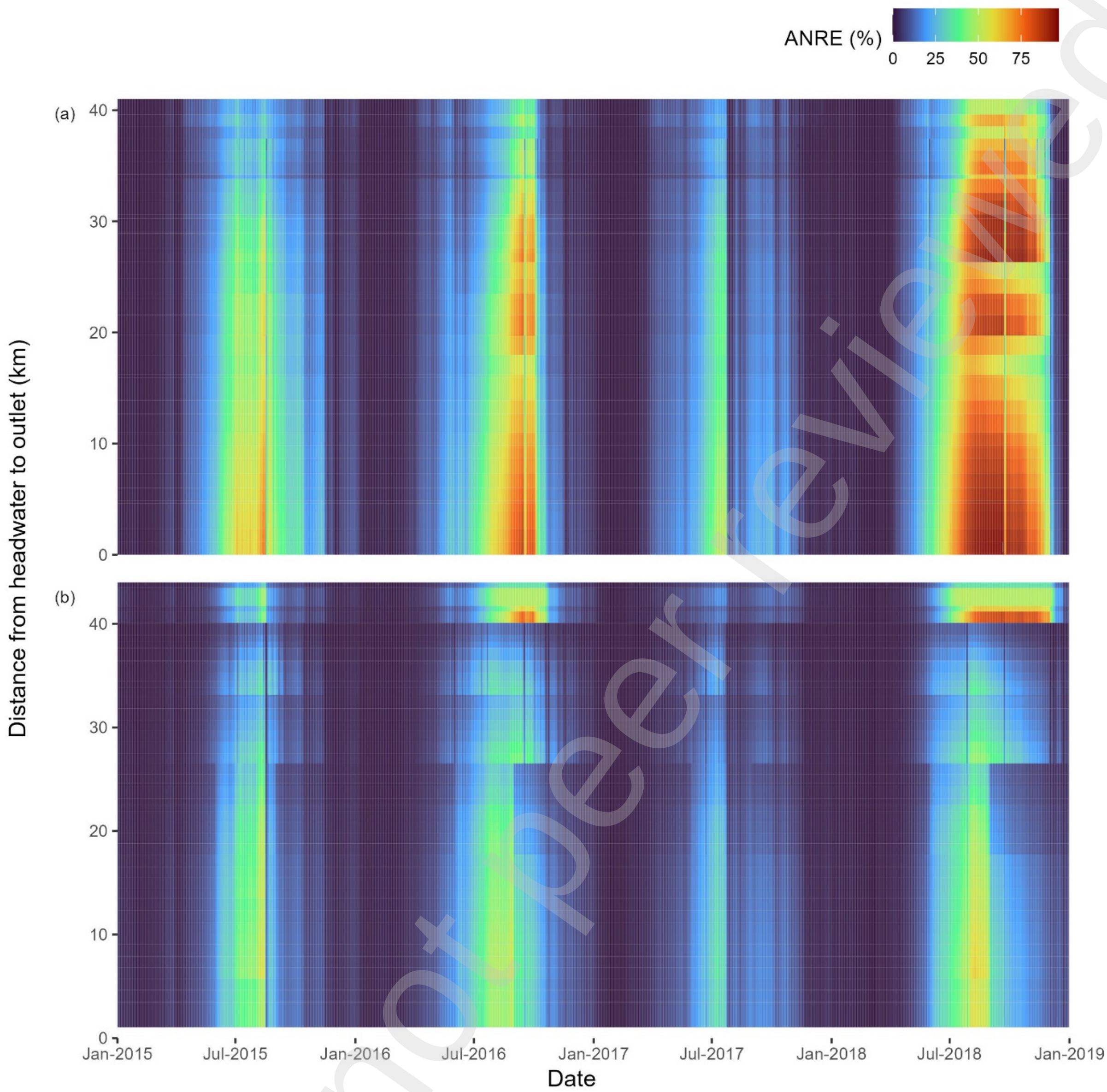


**Figure 4.** Patterns of accumulated net retention efficiency (ANRE) in the (a) Upper Selke and (b) Großer Graben sub-catchments. The y-axis depicts the direction of flow (headwater to outlet = top to bottom), while the x-axis depicts changes over time.

## 3.3 Simulated effects of stream restoration

In the baseline scenario, summer net nitrate retention efficiency ($Eff_{net}$) was slightly higher in streams in forested areas versus agricultural areas (median = 6.2% vs. 3.9%, respectively). Within areas with similar land use, this variable had larger values in small streams than in large streams. For example, in the summer in Großer Graben, the values of $Eff_{net}$ ranged from 0.1 to 34.0% for 1st–3rd order streams and from 0.1 to 2.0% for 4th–5th order streams (Figure 5a). In the restoration scenario, in the summer, greater improvements in net retention efficiency were seen for small streams in Großer Graben (1st–3rd order streams: increase of 0.1–16.8%, 4th–5th order streams: increase of 0–11.8%) (Figure 5b). The most dramatic increase (25.4%) was seen for a 1st-order stream (Figure 5b).

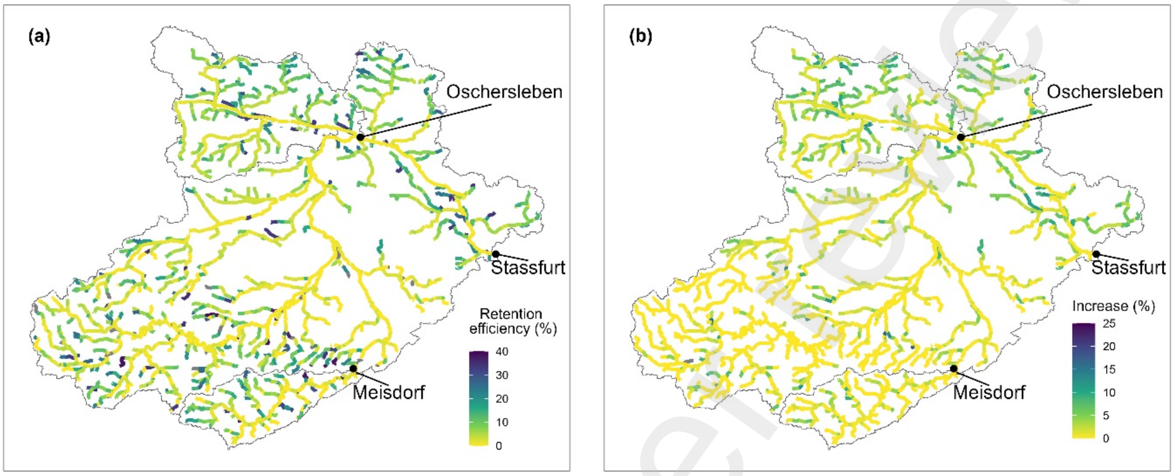


**Figure 5.** Spatial patterns of net nitrate retention efficiency in the summer in the a) baseline scenario and (b) in the restoration scenario (% increase over baseline).

In the baseline scenario, within areas with similar land use, mean summer nitrate concentrations were higher in small streams (1st–3rd order) than in large streams (4th–6th order) (Figure 6a). For instance, in Großer Graben, the range for small streams was 3.3–4.8 mg N $L^{-1}$, while the range for large streams was 2.3–2.6 mg N $L^{-1}$. Additionally, these concentrations were also higher in small streams found in lowland agricultural areas (range = 0.9–17.0 mg N $L^{-1}$) than in small streams in mountainous areas (range = 0.6–5.2 mg N $L^{-1}$) (Figure 6a). In the restoration scenario, nitrate concentrations declined more sharply in the former than in the latter areas; the largest decrease occurred in the tributaries of the lower Bode river (-1.3 mg N $L^{-1}$; Figure 6b). In lowland areas, summer nitrate concentrations dropped more for large streams (4th–6th order) than for small streams (1st–3rd order) (Figures 6b and S7b). For example, in Großer Graben, these concentrations declined by 0.1–0.3 mg N $L^{-1}$ and 0.3-0.5 mg N $L^{-1}$ for small and large streams, respectively.

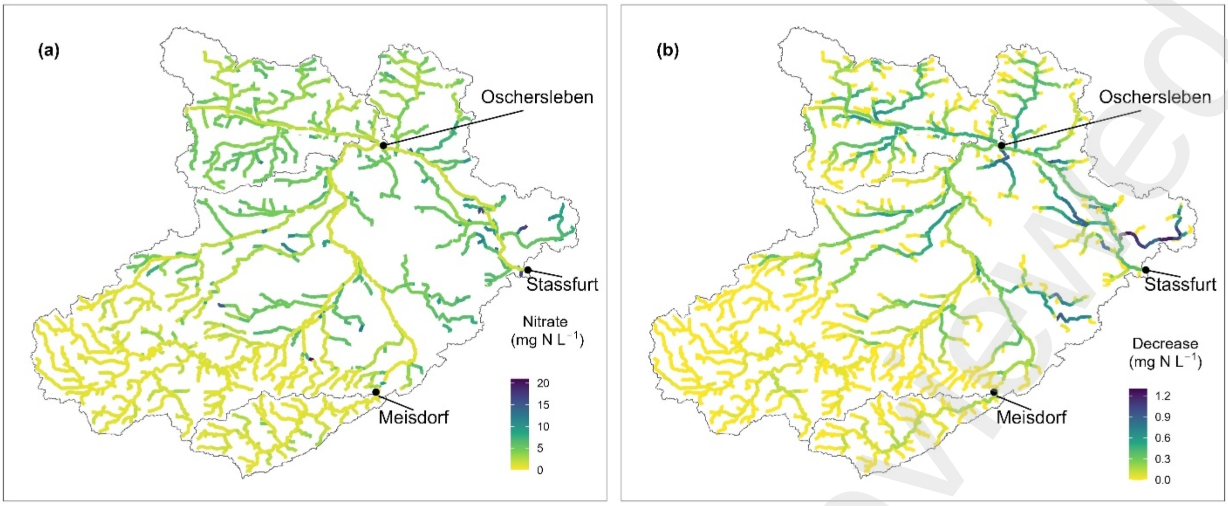


**Figure 6.** Spatial patterns of mean summer nitrate concentrations in the a) baseline scenario and (b) in the restoration scenario (absolute decrease from baseline).

# 4. Discussion

In this study, we investigated the potential effects of stream restoration on nitrate retention dynamics via a combined approach. We utilized the detailed monitoring data available for the Bode catchment in a well-calibrated, process-based mHM-Nitrate model to explore network-scale patterns. According to established criteria for evaluating watershed model performance (Moriasi et al., 2015; Moriasi et al., 2012), the mHM-Nitrate model generally performed well in capturing the dynamics of both discharge and nitrate concentrations. Although the model struggled somewhat with discharge at the Meisdorf and Nienhagen stations (PBIAS: 23.8% and 36.1%, respectively; Table 2), the absolute differences between the observed and estimated values were small (Meisdorf: 36.1 mm year$^{-1}$ and Nienhagen: 23.5 mm year$^{-1}$). Nitrate concentrations were overestimated at the Oschersleben station for the entire modeling period (2010–2018) because discharge and nitrate concentrations were overestimated (PBIAS: 26.8% and 18.4%, respectively) in the summer during the validation period. The differences corresponded to 3.34 mm year$^{-1}$ and 0.31 mg N L$^{-1}$, respectively. A detailed discussion of model performance for the Bode catchment is provided by Zhou et al. (2022).

## 4.1 Modeling nitrate retention processes in stream networks

The mHM-Nitrate model estimated that, in the summer, daily denitrification rates ($U_{den}$) ranged from 100.9 to 198.5 mg N m$^{-2}$ d$^{-1}$ (mean ± SD = 151.1 ± 19.1 mg N m$^{-2}$ d$^{-1}$ for the entire stream network). These figures fit with those obtained by Mulholland et al. (2009), who used $^{15}$N isotope analysis to estimate daily denitrification rates ($U_{den}$) at the reach scale. They found that values ranged from 0 to 220.1 mg N m$^{-2}$ d$^{-1}$ for small streams in areas with different land uses and climatic conditions. Using a reach-scale $N_2$ method on N-enriched streams, Böhlke et al. (2009) estimated that daily denitrification rates ($U_{den}$) in the Iroquois River basin (USA) ranged from 48.4 to 677.0 mg N m$^{-2}$ d$^{-1}$; stream nitrate concentrations were similar between their study and ours. In addition, Zhang et al. (2023) used high-frequency measurements to quantify daily denitrification rates ($U_{den}$) in the summer in the lower Bode River. These observed values fell between 72.3 and 253.0 mg N m$^{-2}$ d$^{-1}$ and were thus reasonably similar to our model's estimated values of 81.8 to 188.2 mg N m$^{-2}$ d$^{-1}$ for the same reaches.

The model estimated that daily assimilatory uptake rates ($U_{assim}$) were $\mathbf{27.6 \pm 24.3}$ and $\mathbf{102.0 \pm 77.5}$ mg N m$^{-2}$ d$^{-1}$ for streams in forested and agricultural areas, respectively (Table 4). Using high-frequency measurements, Rode et al. (2016) found maximum daily assimilatory uptake rates in a Selke sub-catchment (streams in forested areas: 97.5 mg N m$^{-2}$ d$^{-1}$ and streams in agricultural areas: 270 mg N m$^{-2}$ d$^{-1}$) that are consistent with our results (Figure 3 and Table 4). Applying the same model to the Selke catchment, Yang et al. (2019) reported values ($mean \pm SD$) of $\mathbf{86.4 \pm 1.9}$ mg N m$^{-2}$ d$^{-1}$ for streams in forested areas and $\mathbf{18.8 \pm 6.2}$ mg N m$^{-2}$ d$^{-1}$ for streams in agricultural areas. Kunz et al. (2017b) determined that mean daily assimilatory uptake rates ($U_{assim}$) were 120 mg N m$^{-2}$ d$^{-1}$ and 239 mg N m$^{-2}$ d$^{-1}$ for channelized and natural streams, respectively. This work took place in the lowlands associated with the Weiße Elster River, which is near to our study area and thus provides additional support for the reliability of our model's estimates.

## 4.2 Relationships between catchment characteristics and nitrate retention

Nitrate retention is determined by both denitrification and assimilatory uptake ($U_{den}$ and $U_{assim}$). These variables displayed pronounced seasonal variability among different land-use categories (Figure 3). Denitrification ($U_{den}$) was higher in the summer and autumn and lower in the spring and winter for both sub-catchments. This pattern matches those seen in previous studies (Alexander et al., 2009; Wollheim et al., 2008), where retention dynamics were correlated with nitrate concentrations and temperature. This seasonality could also be related to levels of sediment and dissolved oxygen (Christensen et al., 1990; Inwood et al., 2005; Uusheimo et al., 2018) and to levels of organic carbon (Arango et al., 2007; Comer-Warner et al., 2020; Tatariw et al., 2013). However, we were unable to include these variables in our mHM-Nitrate model because the lack of observed data made it impossible to construct empirical equations that would have allowed us to scale up to the entire stream network.

From 2015 to 2018, denitrification rates ($U_{den}$) were higher in Großer Graben than in Upper Selke across all seasons (Figure 3 and Table 4). This pattern likely resulted from the higher nitrate$^-$ concentrations and water temperatures in Großer Graben, a sub-catchment dominated by agricultural activity. Our findings concur with those of past studies (Böhlke et al. (2009); Inwood et al. (2007); Mulholland et al. (2008)), which observed that denitrification rates ($U_{den}$) were positively correlated with nitrate concentrations across land use types.

Assimilatory uptake rates ($U_{assim}$) were similarly higher in Großer Graben than in Upper Selke across all seasons (Figure 3 and Table 4). These results align with those of previous research that utilized high-frequency measurements (Rode et al. 2016) and that applied the mHM-Nitrate model to the Selke catchment (Yang et al., 2019a). The latter two studies reported that assimilatory uptake ($U_{assim}$) occurred at a higher rate in streams in open-canopy environments (i.e., agricultural areas) versus closed-canopy environments (i.e., forests). Arango et al. (2008) found similar results. The assimilatory uptake of nitrate is mainly controlled by primary productivity (Heffernan and Cohen, 2010; Roberts and Mulholland, 2007), which is affected by light, a resource whose availability is higher in agricultural versus forested areas (Yang et al., 2019). Denitrification always peaked after assimilatory uptake, in the second half of July and August. This pattern likely arises because denitrification is more sensitive to water temperature, while assimilatory uptake is more sensitive to light availability (Heffernan and Cohen, 2010, Kunz et al. 2017b). Dynamics were consistent across streams and years.

Although the rates of both processes varied in space and time for the two sub-catchments, denitrification surpassed assimilatory uptake across all seasons, except for spring. Our observation fits with the work by Böhlke et al. (2004), who noted that denitrification accounted for more than 50% of gross nitrate uptake in a stream with high nitrate concentrations (i.e., occurring in an agricultural area). Similarly, Potter et al. (2010) reported that denitrification accounted for 1–97% of gross nitrate uptake and that this figure exceeded 35% for five out of the nine streams studied. Kunz et al. (2017b) found that, in July, the denitrification rate was about five times higher than the assimilatory uptake rate in a natural reach of the Weiße Elster River. In contrast, Mulholland et al. (2008) indicated that denitrification made a relatively limited contribution (16%) to gross nitrate uptake (mainly in low-nitrate streams); Ribot et al. (2017) arrived at a figure of 0.15%. These low values may have resulted from specific site conditions. They were obtained using $^{15}NO_3^-$ tracers that were added to streams with low nitrate concentrations. It appears that denitrification makes a greater contribution to total nitrate uptake when nitrate concentrations are higher.

Upper Selke and Großer Graben likely had similar temporal patterns of gross nitrate retention efficiency and ANRE (Figures 3 and 4) because of similarities in interactions among land use, nitrate concentrations, temperature, and discharge. Both variables had low values in the winter and spring due to elevated terrestrial inputs during high flow periods, and seasonally low water temperatures resulted in reduced rates of assimilatory uptake and denitrification (Alexander et al., 2009). Terrestrial inputs likely had more influence on the above temporal dynamics because they were an order of magnitude larger. While terrestrial inputs were higher in Großer Graben than Upper Selke, median gross nitrate retention efficiency in the summer was higher in Großer Graben than Upper Selke (Table 4), a pattern that can be explained by the former's higher rates of assimilatory uptake and denitrification. The sub-catchments displayed significantly different spatial patterns of ANRE (Figure 4). ANRE was low in Upper Selke headwaters because assimilatory uptake and denitrification were low (Figure 4a); it was higher in Großer Graben headwaters than downstream reaches (Figure 4b) because the elevated nitrate levels caused by terrestrial inputs in the downstream reaches far exceeded the amounts of nitrate removed by assimilatory uptake and denitrification. This result indicates that land use around the nitrate source (e.g., arable land) can strongly influence retention efficiency at the network scale. Previous research arrived at a similar conclusion: land use, and notably the location of arable lands within catchments, can strongly affect the nitrate removal and export from the catchment (Casquin et al., 2021; Dupas et al., 2019; Mineau et al., 2015).

### 4.3 Potential effects of restoring sinuosity on nitrate retention

In our baseline scenario, summer net nitrate retention efficiency was higher in streams in forested versus agricultural areas (Figure 5a). Indeed, in the latter, retention capacity was overwhelmed by large nitrate inputs from terrestrial sources. Adjusting for stream length, net nitrate retention efficiency per km was lower for large than small streams (Figure 5a), as seen in previous studies (Wollheim et al., 2008; Wollheim et al., 2006).

Our restoration scenario specifically explored the effects of increasing stream sinuosity. It found that in areas with arable land, the changes to stream morphology increased net nitrate retention efficiency more in the lowlands than in the mountains (Figure 5b); in the latter area, small streams already display pronounced meandering (Figure S3). As stream length increased, so did the benthic surface areas, also augmenting retention. These gains have also been observed at the reach scale in prior research (Wagenschein and Rode, 2008).

Furthermore, in our restoration scenario, net nitrate retention efficiency improved more for small streams ($1^{st}$–$3^{rd}$ order) than for large streams ($4^{th}$–$6^{th}$ order), as seen in Großer Graben (Figure 5b). This pattern emerges because terrestrial nitrate input greatly exceeds nitrate retention in larger streams, which suggests that increasing sinuosity could have a greater impact on retention efficiency in small streams. Across the entire stream network, increased sinuosity more dramatically reduced nitrate concentrations in large streams than in small streams (Figure 6b), likely because large streams have experienced cumulative downstream retention and harbor larger benthic surface areas (Alexander et al., 2009). Consequently, restoration regimes that increase sinuosity could be powerfully deployed in small streams in agricultural areas, acting to increase nitrate retention efficiency and decrease nitrate transport downstream.

Our study adds to research looking at how alterations in stream morphology could affect nitrate retention dynamics. Past work has shown that re-meandering can induce transient storage, which impacts the denitrification rate (Baker et al., 2012; Opdyke et al., 2006). Such may result mechanistically from lower flow velocities and higher water residence times in the hyporheic zone (Bukaveckas, 2007; Gomez et al., 2012; Pinay et al., 2009; Zarnetske et al., 2011). Additionally, denitrification could experience greater increase in vertical hyporheic zones compared to meanders because vertical exchanges beneath stream bedforms are considerably more pronounced than are lateral exchanges through stream bars and meander banks (Gomez-Velez and Harvey, 2014; Gomez-Velez et al., 2015). Modifications to stream morphology can directly or indirectly affect nutrient dynamics by increasing spatiotemporal variability in the composition and activity of aquatic communities (Lin et al., 2016). However, it is hard to arrive at any generalizations because we continue to lack field studies comparing denitrification rates in modified versus natural streams—data that are essential for model parameterization. We have interpreted our results conservatively because we did not explicitly establish any links between these processes and natural stream morphology, which shapes rates of nitrate uptake in the stream bed.

### 4.4 Implications for stream restoration

Although stream restoration projects are abundant, they often focus on the reach scale (Newcomer Johnson et al., 2016). This study highlights the need for developing methods that act at the network scale, such as increasing stream sinuosity. In our simulation, increasing stream sinuosity improved nitrate retention efficiency more in streams in agricultural areas (Großer Graben) than in streams in forested areas (Upper Selke). Moreover, this strategy more dramatically reduced nitrate concentrations in large streams than in small streams because of the accumulative retention in the upper streams. This finding indicates that restoration efforts should prioritize small streams in highly polluted, agricultural areas, such as our study area in the lowlands of central Germany.

Encouraging investment in stream restoration (e.g., re-meandering) can be challenging for two key reasons: first, it is costly and technically difficult and, second, the benefits are only significant during periods of low flow and low terrestrial inputs. Realistically, stream restoration alone cannot reduce nitrate concentrations to desired levels. Instead, systems exploiting a combination of terrestrial and stream-targeted measurements could be used to effectively and sustainably manage river basins (Lammers and Bledsoe, 2017). However, we must first conduct further research on how such combined measurements can affect nitrate retention at the stream network scale.

# 5. Conclusion

In this study, we used observed data from Germany's Bode catchment in combination with a fully distributed process-based mHM-Nitrate model to investigate how re-meandering could affect nitrate retention dynamics within a heavily modified stream network. There was pronounced spatiotemporal variability in rates of assimilatory uptake and denitrification within stream networks with different land-use types and morphological characteristics. Both rates were higher in streams in more agricultural versus more forested areas. At the network scale, increased stream sinuosity had a greater positive impact on nitrate retention efficiency in small streams. However, nitrate concentrations decreased more dramatically in large streams due to accumulative retention in upper streams. Our findings underscore that major benefits could arise from re-meandering small streams in agricultural areas. It is important to acknowledge that our stream restoration regime was somewhat simplified—we increased sinuosity without considering the resulting effects on rates of nitrate denitrification and assimilatory uptake. Thus, this work is a conservative first step along a lengthy research pathway. For example, future research should explore whether nitrate retention efficiency could be enhanced even more by combining stream-based strategies (e.g., re-meandering, improved floodplain connectivity) with land-based strategies (e.g., buffer strips, construction of wetlands).

Our results highlight the dominant role of denitrification in gross nitrate uptake across all seasons (excluding the spring). They also showed that, regardless of stream size or nearby land use, the denitrification rate always peaked after the assimilatory uptake rate, in the second half of July and August.

Taken together, our findings suggest that stream restoration efforts should prioritize small streams in highly polluted, agricultural areas. To optimally design restoration strategies, we must characterize denitrification and assimilatory uptake rates in stream networks in the field before and after restoration; these data could then be used in distributed hydrological water quality models (such as an mHM-Nitrate model) to further improve understanding of these dynamics.

# Acknowledgements

X. Zhou is funded by the Chinese Scholarship Council (CSC). We thank the German Weather Service (DWD), Federal Institute for Geosciences and Natural Resources (BGR) and State Agency for Flood Protection and Water Management of Saxony-Anhalt (LHW) for providing meteorological, geological and discharge and water-quality data, respectively. The high-frequency nitrate-concentration data were provided by the TERENO (Terrestrial Environment Observatories) project.

# References


Agency, E.E. (2018) European waters — assessment of status and pressures 2018.

Alexander, R.B., Bohlke, J.K., Boyer, E.W., David, M.B., Harvey, J.W., Mulholland, P.J., Seitzinger, S.P., Tobias, C.R., Tonitto, C. and Wollheim, W.M. 2009. Dynamic modeling of nitrogen losses in river networks unravels the coupled effects of hydrological and biogeochemical processes. Biogeochemistry 93(1-2), 91-116.

Arango, C.P., Tank, J.L., Schaller, J.L., Royer, T.V., Bernot, M.J. and David, M.B. 2007. Benthic organic carbon influences denitrification in streams with high nitrate concentration. Freshwater Biology 52(7), 1210-1222.

Baker, D.W., Bledsoe, B.P. and Price, J.M. 2012. Stream nitrate uptake and transient storage over a gradient of geomorphic complexity, north-central Colorado, USA. Hydrological Processes 26(21), 3241-3252.

Birgand, F., Skaggs, R.W., Chescheir, G.M. and Gilliam, J.W. 2007. Nitrogen Removal in Streams of Agricultural Catchments—A Literature Review. Critical Reviews in Environmental Science and Technology 37(5), 381-487.

Böhlke, J.K., Antweiler, R.C., Harvey, J.W., Laursen, A.E., Smith, L.K., Smith, R.L. and Voytek, M.A. 2009. Multi-scale measurements and modeling of denitrification in streams with varying flow and nitrate concentration in the upper Mississippi River basin, USA. Biogeochemistry 93(1-2), 117-141.

Böhlke, J.K., Harvey, J.W. and Voytek, M.A. 2004. Reach-scale isotope tracer experiment to quantify denitrification and related processes in a nitrate-rich stream, midcontinent United States. Limnology and Oceanography 49(3), 821-838.

Briem, E., Spitzer, A. and Schrenk, G. 2003. Gewässerlandschaften der Bundesrepublik Deutschland. WASSERWIRTSCHAFT 94, 58-62.

Bukaveckas, P.A. 2007. Effects of channel restoration on water velocity, transient storage, and nutrient uptake in a channelized stream. Environ Sci Technol 41(5), 1570-1576.

Carvalho, L., Mackay, E.B., Cardoso, A.C., Baattrup-Pedersen, A., Birk, S., Blackstock, K.L., Borics, G., Borja, A., Feld, C.K., Ferreira, M.T., Globevnik, L., Grizzetti, B., Hendry, S., Hering, D., Kelly, M., Langaas, S., Meissner, K., Panagopoulos, Y., Penning, E., Rouillard, J., Sabater, S., Schmedtje, U., Spears, B.M., Venohr, M., van de Bund, W. and Solheim, A.L. 2019. Protecting and restoring Europe's waters: An analysis of the future development needs of the Water Framework Directive. Science of The Total Environment 658, 1228-1238.

Casquin, A., Dupas, R., Gu, S., Couic, E., Gruau, G. and Durand, P. 2021. The influence of landscape spatial configuration on nitrogen and phosphorus exports in agricultural catchments. Landscape Ecology 36(12), 3383-3399.

Christensen, P.B., Nielsen, L.P., Sørensen, J. and Revsbech, N.P. 1990. Denitrification in nitrate-rich streams: Diurnal and seasonal variation related to benthic oxygen metabolism. Limnology and Oceanography 35(3), 640-651.

Comer-Warner, S.A., Gooddy, D.C., Ullah, S., Glover, L., Kettridge, N., Wexler, S.K., Kaiser, J. and Krause, S. 2020. Seasonal variability of sediment controls of nitrogen cycling in an agricultural stream. Biogeochemistry 148(1), 31-48.

Covino, T., McGlynn, B. and Baker, M. 2010. Separating physical and biological nutrient retention and quantifying uptake kinetics from ambient to saturation in successive mountain stream reaches. Journal of Geophysical Research 115(G4).

Craig, L.S., Palmer, M.A., Richardson, D.C., Filoso, S., Bernhardt, E.S., Bledsoe, B.P., Doyle, M.W., Groffman, P.M., Hassett, B.A., Kaushal, S.S., Mayer, P.M., Smith, S.M. and Wilcock, P.R. 2008. Stream restoration strategies for reducing river nitrogen loads. Frontiers in Ecology and the Environment 6(10), 529-538.

Doyle, M.W., Stanley, E.H. and Harbor, J.M. 2003. Hydrogeomorphic controls on phosphorus retention in streams. Water Resources Research 39(6).
Dupas, R., Abbott, B.W., Minaudo, C. and Fovet, O. 2019. Distribution of Landscape Units Within Catchments Influences Nutrient Export Dynamics. Frontiers in Environmental Science 7.
Ensign, S.H. and Doyle, M.W. 2006. Nutrient spiraling in streams and river networks. Journal of Geophysical Research: Biogeosciences 111(G4).
European Commission 1991a Council Directive 91/271/EEC of 21 May 1991 concerning urban waste-water treatment.
European Commission 1991b Council Directive 91/676/EEC of 12 December 1991 concerning the protection of waters against pollution caused by nitrates from agricultural sources.
Flávio, H.M., Ferreira, P., Formigo, N. and Svendsen, J.C. 2017. Reconciling agriculture and stream restoration in Europe: A review relating to the EU Water Framework Directive. Science of The Total Environment 596-597, 378-395.
Gomez-Velez, J.D. and Harvey, J.W. 2014. A hydrogeomorphic river network model predicts where and why hyporheic exchange is important in large basins. Geophysical Research Letters 41(18), 6403-6412.
Gomez-Velez, J.D., Harvey, J.W., Cardenas, M.B. and Kiel, B. 2015. Denitrification in the Mississippi River network controlled by flow through river bedforms. Nature Geoscience 8(12), 941-945.
Gomez, J.D., Wilson, J.L. and Cardenas, M.B. 2012. Residence time distributions in sinuosity ‐ driven hyporheic zones and their biogeochemical effects. Water Resources Research 48(9).
Groffman, P.M., Butterbach-Bahl, K., Fulweiler, R.W., Gold, A.J., Morse, J.L., Stander, E.K., Tague, C., Tonitto, C. and Vidon, P. 2009. Challenges to incorporating spatially and temporally explicit phenomena (hotspots and hot moments) in denitrification models. Biogeochemistry 93(1-2), 49-77.
Gucker, B. and Boechat, I.G. 2004. Stream morphology controls ammonium retention in tropical headwaters. Ecology 85(10), 2818-2827.
Guzelj, M., Hauer, C. and Egger, G. 2020. The third dimension in river restoration: how anthropogenic disturbance changes boundary conditions for ecological mitigation. Sci Rep 10(1), 13106.
Harnischmacher, S. 2007. Thresholds in small rivers? Hypotheses developed from fluvial morphological research in western Germany. Geomorphology 92(3-4), 119-133.
Heffernan, J.B. and Cohen, M.J. 2010. Direct and indirect coupling of primary production and diel nitrate dynamics in a subtropical spring-fed river. Limnology and Oceanography.
Helton, A.M., Hall, R.O. and Bertuzzo, E. 2018. How network structure can affect nitrogen removal by streams. Freshwater Biology 63(1), 128-140.
Helton, A.M., Poole, G.C., Meyer, J.L., Wollheim, W.M., Peterson, B.J., Mulholland, P.J., Bernhardt, E.S., Stanford, J.A., Arango, C., Ashkenas, L.R., Cooper, L.W., Dodds, W.K., Gregory, S.V., Hall, R.O., Hamilton, S.K., Johnson, S.L., McDowell, W.H., Potter, J.D., Tank, J.L., Thomas, S.M., Valett, H.M., Webster, J.R. and Zeglin, L. 2011. Thinking outside the channel: modeling nitrogen cycling in networked river ecosystems. Frontiers in Ecology and the Environment 9(4), 229-238.
Huang, J., Borchardt, D. and Rode, M. 2022. How do inorganic nitrogen processing pathways change quantitatively at daily, seasonal, and multiannual scales in a large agricultural stream? Hydrol. Earth Syst. Sci. 26(22), 5817-5833.
Huang, S., Krysanova, V. and Hattermann, F. 2015. Projections of climate change impacts on floods and droughts in Germany using an ensemble of climate change scenarios. Regional Environmental Change 15(3), 461-473.
Inwood, S.E., Tank, J.L. and Bernot, M.J. 2005. Patterns of denitrification associated with land use in 9 midwestern headwater streams. J N Am Benthol Soc 24(2), 227-245.
Inwood, S.E., Tank, J.L. and Bernot, M.J. 2007. Factors controlling sediment denitrification in midwestern streams of varying land use. Microb Ecol 53(2), 247-258.

Kaushal, S.S., Groffman, P.M., Mayer, P.M., Striz, E. and Gold, A.J. 2008. Effects of stream restoration on denitrification in an urbanizing watershed. Ecol Appl 18(3), 789-804.
Klocker, C.A., Kaushal, S.S., Groffman, P.M., Mayer, P.M. and Morgan, R.P. 2009. Nitrogen uptake and denitrification in restored and unrestored streams in urban Maryland, USA. Aquatic Sciences 71(4), 411-424.
Kunz, J.V., Annable, M.D., Cho, J., von Tümpling, W., Hatfield, K., Rao, S., Borchardt, D. and Rode, M. 2017a. Quantifying nutrient fluxes with a new hyporheic passive flux meter (HPFM). Biogeosciences 14(3), 631-649.
Kunz, J.V., Hensley, R., Brase, L., Borchardt, D. and Rode, M. 2017b. High frequency measurements of reach scale nitrogen uptake in a fourth order river with contrasting hydromorphology and variable water chemistry (Weiße Elster, Germany). Water Resources Research 53(1), 328-343.
Kupilas, B., Hering, D., Lorenz, A.W., Knuth, C. and Gücker, B. 2017. Hydromorphological restoration stimulates river ecosystem metabolism. Biogeosciences 14(7), 1989-2002.
Lammers, R.W. and Bledsoe, B.P. 2017. What role does stream restoration play in nutrient management? Critical Reviews in Environmental Science and Technology 47(6), 335-371.
Lin, L., Davis, L., Cohen, S., Chapman, E. and Edmonds, J.W. 2016. The influence of geomorphic unit spatial distribution on nitrogen retention and removal in a large river. Ecological Modelling 336, 26-35.
Lin, L., Reisinger, A.J., Rosi, E.J., Groffman, P.M. and Band, L.E. 2021. Evaluating Instream Restoration Effectiveness in Reducing Nitrogen Export from an Urban Catchment with a Data‐Model Approach. JAWRA Journal of the American Water Resources Association 57(3), 449-473.
Lindström, G., Pers, C., Rosberg, J., Strömqvist, J. and Arheimer, B. 2010. Development and testing of the HYPE (Hydrological Predictions for the Environment) water quality model for different spatial scales. Hydrology Research 41(3-4), 295-319.
Lorenz, A.W., Jahnig, S.C. and Hering, D. 2009. Re-meandering German lowland streams: qualitative and quantitative effects of restoration measures on hydromorphology and macroinvertebrates. Environ Manage 44(4), 745-754.
Marcé, R., von Schiller, D., Aguilera, R., Martí, E. and Bernal, S. 2018. Contribution of Hydrologic Opportunity and Biogeochemical Reactivity to the Variability of Nutrient Retention in River Networks. Global Biogeochemical Cycles 32(3), 376-388.
Mineau, M.M., Wollheim, W.M. and Stewart, R.J. 2015. An index to characterize the spatial distribution of land use within watersheds and implications for river network nutrient removal and export. Geophysical Research Letters 42(16), 6688-6695.
Ministerium für Umwelt und Naturschutz Landwirtschaft und Verbraucherschutz des Landes Nordrhein-Westfalen (2010) Richtlinie für die Entwicklung naturnaher Fließgewässer in Nordrhein-Westfalen: Ausbau und Unterhaltung,Düsseldorf https://www.lanuv.nrw.de/fileadmin/lanuvpubl/6_sonderreihen/60007.pdf.
Moriasi, D.N., Gitau, M.W., Pai, N. and Daggupati, P. 2015. Hydrologic and Water Quality Models: Performance Measures and Evaluation Criteria. Transactions of the Asabe 58(6), 1763-1785.
Moriasi, D.N., Wilson, B.N., Douglas-Mankin, K.R., Arnold, J.G. and Gowda, P.H. 2012. Hydrologic and Water Quality Models: Use, Calibration, and Validation. Transactions of the Asabe 55(4), 1241-1247.
Mueller, C., Zink, M., Samaniego, L., Krieg, R., Merz, R., Rode, M. and Knoller, K. 2016. Discharge Driven Nitrogen Dynamics in a Mesoscale River Basin As Constrained by Stable Isotope Patterns. Environ Sci Technol 50(17), 9187-9196.
Mulholland, P.J., Hall Jr, R.O., Sobota, D.J., Dodds, W.K., Findlay, S.E., Grimm, N.B., Hamilton, S.K., McDowell, W.H., O'Brien, J.M. and Tank, J.L. 2009. Nitrate removal in stream ecosystems measured by 15N addition experiments: denitrification. Limnology and Oceanography 54(3), 666-680.
Mulholland, P.J., Helton, A.M., Poole, G.C., Hall, R.O., Hamilton, S.K., Peterson, B.J., Tank, J.L., Ashkenas, L.R., Cooper, L.W., Dahm, C.N., Dodds, W.K., Findlay, S.E., Gregory, S.V., Grimm,

N.B., Johnson, S.L., McDowell, W.H., Meyer, J.L., Valett, H.M., Webster, J.R., Arango, C.P., Beaulieu, J.J., Bernot, M.J., Burgin, A.J., Crenshaw, C.L., Johnson, L.T., Niederlehner, B.R., O'Brien, J.M., Potter, J.D., Sheibley, R.W., Sobota, D.J. and Thomas, S.M. 2008. Stream denitrification across biomes and its response to anthropogenic nitrate loading. Nature 452(7184), 202-205.

Newcomer Johnson, T., Kaushal, S., Mayer, P., Smith, R. and Sivirichi, G. 2016. Nutrient Retention in Restored Streams and Rivers: A Global Review and Synthesis. Water 8(4).

Opdyke, M.R., David, M.B. and Rhoads, B.L. 2006. Influence of geomorphological variability in channel characteristics on sediment denitrification in agricultural streams. J Environ Qual 35(6), 2103-2112.

Pander, J., Mueller, M., Knott, J., Egg, L. and Geist, J. 2017. Is it Worth the Money? The Functionality of Engineered Shallow Stream Banks as Habitat for Juvenile Fishes in Heavily Modified Water Bodies. River Research and Applications 33(1), 63-72.

Passy, P., Garnier, J., Billen, G., Fesneau, C. and Tournebize, J. 2012. Restoration of ponds in rural landscapes: modelling the effect on nitrate contamination of surface water (the Seine River Basin, France). Sci Total Environ 430, 280-290.

Pedersen, M.L., Kristensen, K.K. and Friberg, N. 2014. Re-meandering of lowland streams: will disobeying the laws of geomorphology have ecological consequences? PLoS One 9(9), e108558.

Pinay, G., O'Keefe, T.C., Edwards, R.T. and Naiman, R.J. 2009. Nitrate removal in the hyporheic zone of a salmon river in Alaska. River Research and Applications 25(4), 367-375.

Potter, J.D., McDowell, W.H., Merriam, J.L., Peterson, B.J. and Thomas, S.M. 2010. Denitrification and total nitrate uptake in streams of a tropical landscape. Ecol Appl 20(8), 2104-2115.

Rhoads, B.L. 2010. Stream Power Terminology. The Professional Geographer 39(2), 189-195.

Ribot, M., von Schiller, D. and Martí, E. 2017. Understanding pathways of dissimilatory and assimilatory dissolved inorganic nitrogen uptake in streams. Limnology and Oceanography 62(3), 1166-1183.

Roberts, B.J. and Mulholland, P.J. 2007. In-stream biotic control on nutrient biogeochemistry in a forested stream, West Fork of Walker Branch. Journal of Geophysical Research: Biogeosciences 112(G4).

Rode, M., Halbedel Nee Angelstein, S., Anis, M.R., Borchardt, D. and Weitere, M. 2016. Continuous In-Stream Assimilatory Nitrate Uptake from High-Frequency Sensor Measurements. Environ Sci Technol 50(11), 5685-5694.

Roley, S.S., Tank, J.L. and Williams, M.A. 2012. Hydrologic connectivity increases denitrification in the hyporheic zone and restored floodplains of an agricultural stream. Journal of Geophysical Research: Biogeosciences 117(G3).

Samaniego, L., Kumar, R. and Attinger, S. 2010. Multiscale parameter regionalization of a grid-based hydrologic model at the mesoscale. Water Resources Research 46(5).

Tatariw, C., Chapman, E.L., Sponseller, R.A., Mortazavi, B. and Edmonds, J.W. 2013. Denitrification in a large river: consideration of geomorphic controls on microbial activity and community structure. Ecology 94(10), 2249-2262.

Uusheimo, S., Tulonen, T., Aalto, S.L. and Arvola, L. 2018. Mitigating agricultural nitrogen load with constructed ponds in northern latitudes: A field study on sedimental denitrification rates. Agriculture, Ecosystems & Environment 261, 71-79.

Veraart, A.J., Audet, J., Dimitrov, M.R., Hoffmann, C.C., Gillissen, F. and de Klein, J.J.M. 2014. Denitrification in restored and unrestored Danish streams. Ecological Engineering 66, 129-140.

Wagenschein, D. and Rode, M. 2008. Modelling the impact of river morphology on nitrogen retention—A case study of the Weisse Elster River (Germany). Ecological Modelling 211(1-2), 224-232.

Wohl, E., Lane, S.N. and Wilcox, A.C. 2015. The science and practice of river restoration. Water Resources Research 51(8), 5974-5997.
Wollheim, W.M., Peterson, B.J., Thomas, S.M., Hopkinson, C.H. and Vörösmarty, C.J. 2008. Dynamics of N removal over annual time periods in a suburban river network. Journal of Geophysical Research 113(G3).
Wollheim, W.M., Vörösmarty, C.J., Peterson, B.J., Seitzinger, S.P. and Hopkinson, C.S. 2006. Relationship between river size and nutrient removal. Geophysical Research Letters 33(6).
Wollschläger, U., Attinger, S., Borchardt, D., Brauns, M., Cuntz, M., Dietrich, P., Fleckenstein, J.H., Friese, K., Friesen, J., Harpke, A., Hildebrandt, A., Jäckel, G., Kamjunke, N., Knöller, K., Kögler, S., Kolditz, O., Krieg, R., Kumar, R., Lausch, A., Liess, M., Marx, A., Merz, R., Mueller, C., Musolff, A., Norf, H., Oswald, S.E., Rebmann, C., Reinstorf, F., Rode, M., Rink, K., Rinke, K., Samaniego, L., Vieweg, M., Vogel, H.-J., Weitere, M., Werban, U., Zink, M. and Zacharias, S. 2016. The Bode hydrological observatory: a platform for integrated, interdisciplinary hydro-ecological research within the TERENO Harz/Central German Lowland Observatory. Environmental Earth Sciences 76(1).
Wu, S., Tetzlaff, D., Yang, X. and Soulsby, C. 2022. Disentangling the Influence of Landscape Characteristics, Hydroclimatic Variability and Land Management on Surface Water NO3 ‐ N Dynamics: Spatially Distributed Modeling Over 30 yr in a Lowland Mixed Land Use Catchment. Water Resources Research 58(2).
Yang, X., Jomaa, S., Buttner, O. and Rode, M. 2019. Autotrophic nitrate uptake in river networks: A modeling approach using continuous high-frequency data. Water Res 157, 258-268.
Yang, X., Jomaa, S., Zink, M., Fleckenstein, J.H., Borchardt, D. and Rode, M. 2018. A New Fully Distributed Model of Nitrate Transport and Removal at Catchment Scale. Water Resources Research.
Yang, X. and Rode, M. 2020 A Fully Distributed Catchment Nitrate Model - mHM-Nitrate v2.0.
Ye, S., Covino, T.P., Sivapalan, M., Basu, N.B., Li, H.-Y. and Wang, S.-W. 2012. Dissolved nutrient retention dynamics in river networks: A modeling investigation of transient flows and scale effects. Water Resources Research 48(6).
Zarnetske, J.P., Haggerty, R., Wondzell, S.M. and Baker, M.A. 2011. Dynamics of nitrate production and removal as a function of residence time in the hyporheic zone. Journal of Geophysical Research 116(G1).
Zhang, X., Yang, X., Hensley, R., Lorke, A. and Rode, M. 2023. Disentangling In ‐ Stream Nitrate Uptake Pathways Based on Two ‐ Station High ‐ Frequency Monitoring in High ‐ Order Streams. Water Resources Research 59(3), e2022WR032329.
Zhou, X., Jomaa, S., Yang, X., Merz, R., Wang, Y. and Rode, M. 2022. Exploring the relations between sequential droughts and stream nitrogen dynamics in central Germany through catchment-scale mechanistic modelling. Journal of Hydrology 614, 128615.